

# Multi-omics analysis of right ventricles in rat models of pulmonary arterial hypertension: Consideration of mitochondrial biogenesis by chrysin

TAKAYUKI KOBAYASHI<sup>1\*</sup>, JUN-DAL KIM<sup>2-4\*</sup>, AKIRA NAITO<sup>1</sup>, ASAKO YANAGISAWA<sup>1</sup>,  
TAKAYUKI JUJO-SANADA<sup>1</sup>, YOSHITOSHI KASUYA<sup>5</sup>, YOSHIMI NAKAGAWA<sup>2</sup>,  
SEIICHIRO SAKAO<sup>1</sup>, KOICHIRO TATSUMI<sup>1</sup> and TAKUJI SUZUKI<sup>1</sup>

<sup>1</sup>Department of Respiriology, Graduate School of Medicine, Chiba University, Chiba 260-8670;

<sup>2</sup>Division of Complex Biosystem Research, Department of Research and Development, Institute of National Medicine, University of Toyama, Toyama 930-0194; <sup>3</sup>Life Science Center for Survival Dynamics, Tsukuba Advanced Research Alliance, University of Tsukuba, Ibaraki 305-8577; <sup>4</sup>Japan Agency for Medical Research-Core Research for Evolution Science and Technology, Tokyo 100-0004; <sup>5</sup>Department of Biomedical Science, Graduate School of Medicine, Chiba University, Chiba 260-8670, Japan

Received December 6, 2021; Accepted February 21, 2022

DOI: 10.3892/ijmm.2022.5124

**Abstract.** In pulmonary arterial hypertension (PAH), right ventricular failure is accompanied by metabolic alterations in cardiomyocytes, which may be due to mitochondrial dysfunction and decreased energy production. Chrysin (CH) is a phytochemical with pharmacological activity that is involved in the regulation of mitochondrial biogenesis. The present study investigated the role of CH in the right ventricle (RV) by analyzing the cardiac transcriptome and metabolome of a SU5416(a vascular endothelial growth factor receptor blocker)/hypoxia (Su/Hx) rat model of PAH. RNA-sequencing of the RV transcriptome between Su/Hx, Su/Hx with CH (Su/Hx + CH) and control groups, extracellular matrix (ECM)

organization and ECM-receptor interaction-associated genes were upregulated in the RV of Su/Hx but not Su/Hx + CH rats. Furthermore, expression of mitochondrial function-, energy production-, oxidative phosphorylation- and tricarboxylic acid (TCA) cycle-associated genes was decreased in the RV of Su/Hx rats; this was reverse by CH. Metabolomic profiling analysis of Su/Hx and Su/Hx + CH rats showed no significant changes in glycolysis, TCA cycle, glutathione, NADH or NADPH. By contrast, in the RV of Su/Hx rats, decreased adenylate energy charge was partially reversed by CH administration, suggesting that CH was involved in the improvement of mitochondrial biogenesis. Reverse transcription-quantitative PCR analysis revealed that expression of peroxisome proliferator-activated receptor  $\gamma$ , a master regulator of fatty acid metabolism and mitochondrial biogenesis, was increased in the RV of Su/Hx + CH rats. CH ameliorated cardiac abnormality, including cardiac fibrosis, RV hypertrophy and PH. The present study suggested that CH altered patterns of gene expression and levels of mitochondrial metabolites in cardiomyocytes, thus improving RV dysfunction in a Su/Hx PAH rat model.

*Correspondence to:* Dr Akira Naito, Department of Respiriology, Graduate School of Medicine, Chiba University, 1-8-1 Inohana, Chuo-Ku, Chiba 260-8670, Japan  
E-mail: akira-n.390@chiba-u.jp

\*Contributed equally

**Abbreviations:** Cpt1b, carnitine palmitoyl transferase 1B; Drp1, dynamin-related protein 1; Ea, arterial elastance; ECM, extracellular matrix; Ees, end-systolic elastance; LC-TOFMS, liquid chromatography time-of-flight mass spectrometry; Mfn, mitofusin; Opal, optic atrophy 1; PAH, pulmonary arterial hypertension; PPAR $\gamma$ , peroxisome proliferator-activated receptor  $\gamma$ ; RVSP, right ventricle systolic pressure; Su/Hx, SU5416 followed by chronic hypoxia; Su/Hx + CH, SU5416 followed by chronic hypoxia and chrysin administration; Tfam, mitochondrial transcription factor A

**Key words:** chrysin, RNA sequencing, metabolome analysis, pulmonary hypertension, right heart, SU5416

## Introduction

Pulmonary arterial hypertension (PAH) is a progressive disease characterized by pulmonary vascular remodeling, leading to increased pulmonary vascular resistance and right ventricle (RV) hypertrophy, resulting in RV failure (1). Although PAH is considered to be a disease of the lungs, RV adaptation to high PA pressure is the most important determinant of prognosis and right heart failure remains a predominant cause of death in PAH (2). RV dysfunction is a complex process that leads to cardiomyocyte hypertrophy, fibrosis, inflammation and metabolic change, such as increased glycolysis (3-6). However, the underlying molecular mechanism of adverse RV remodeling

and dysfunction is poorly understood and, to the best of our knowledge, there are currently no approved therapies that improve RV function.

Flavonoids are natural products found in plants and exhibit diverse biological activity and are involved in regulation of cell cycle, DNA repair and metabolic gene expression (7). Moreover, flavonoids exert pharmacological effects, such as anti-cancer, anti-oxidation and anti-inflammatory effects (8). Chrysin (5,7-dihydroxyflavone; CH), a phytochemical, is one of the most active flavonoids and has been shown to exert cardio-protective effects via its antioxidant and anti-inflammatory activity in multiple experimental models, including myocardial ischemia-reperfusion injury and hypoxic rats (9,10). Recent study suggested that CH attenuates bleomycin-induced pulmonary fibrosis via anti-inflammatory and anti-oxidative effects and the activity of CH as a peroxisome proliferator-activated receptor  $\gamma$  (PPAR- $\gamma$ ) agonist has direct protective effects against inflammation and oxidative stress (11). Therefore, it was hypothesized that CH may exert a therapeutic effect in PAH.

The SU5416/hypoxia (Su/Hx) protocol is based on blockade of vascular endothelial growth factor receptor via tyrosine kinase inhibitor Su and is commonly used to induce animal models of PAH (12,13). In the Su/Hx model, animals receive a single subcutaneous injection of Su in combination with chronic exposure to Hx followed by normoxia, resulting in severe PAH. Therefore, Su/Hx models have been considered as a key preclinical model of PAH due to formation of occlusive pulmonary vascular lesions in the lung and RV dysfunction with marked cardiac hypertrophy, which resembles human idiopathic PAH (14,15).

To determine the molecular mechanisms underlying the effects of PH and CH on RV, gene expression changes in RV of Su/Hx model rats in the presence and absence of CH were analyzed via RNA sequencing (RNA-seq). Metabolomic profiling of RVs was performed to determine metabolic regulation by CH. Pathophysiological changes in Su/Hx + CH PAH rats were observed and pressure-volume curve was constructed using a Millar catheter.

## Materials and methods

**Experimental design and animals.** A total of 30 5-week-old male Sprague-Dawley rats weighing 130–150 g were purchased from Japan SLC (Shizuoka, Japan). All rats were housed in the animal experimental facility of Chiba University and had free access to drinking water and food. The rats were kept at 24°C under a 12 h light/dark cycle in the animal experimental facility of Chiba University as described previously (16). All animal procedures were approved by the Review Board for Animal Experiments of Chiba University (approval no. 30-126) and were performed in accordance with the guidelines of the Animal Research Committee of Laboratory Animal Center, Graduate School of Medicine, Chiba University (17). The rats were divided into three groups (n= 10 rats per group) as follows: i) Untreated control (CTRL); ii) Su/Hx + vehicle (PBS) and iii) Su/Hx + CH administration (Fig. 1).

**Su/Hx rat model and CH administration.** The Su/Hx rat model was established as previously described (18,19). Briefly, Su

(20 mg/kg; R&D Systems, Inc.), a vascular endothelial growth factor receptor inhibitor, was dissolved in 1 ml carboxymethyl cellulose and the suspension was subcutaneously injected into rats. The rats were maintained under normobaric Hx (10% O<sub>2</sub>) for 3 weeks then returned to normoxic conditions (21% O<sub>2</sub>) for 2 weeks.

CH was obtained from Santa Cruz Biotechnology, Inc., dissolved in PBS and administered to Su/Hx rats (100 mg/kg) once/day for 3 weeks, beginning at the end of the 2 week normoxic period (Fig. 1).

**RNA-seq.** A total of ~500 ng total RNA from the heart and lung was ribosomal RNA-depleted using the NEBNext rRNA Depletion kit and converted to an Illumina sequencing library using the NEBNext Ultra Directional RNA Library Prep kit for Illumina (both New England BioLabs, Inc.). The libraries were validated using a Bioanalyzer (Agilent Technologies, Inc.) and 1.5 pM (final loading concentration) of libraries sequenced using the NextSeq 500 (Illumina, Inc.) with the paired-end 36-base read option. Reads were mapped to *Rattus norvegicus* Rnor\_6.0 (rn6) reference genome and quantified using the CLC Genomics Workbench (version 12.0, Qiagen GmbH). RNA-seq datasets were deposited in National Center for Biotechnology Information Gene Expression Omnibus database (ncbi.nlm.nih.gov/geo; accession no. GSE186989).

**Identification of differentially expressed genes (DEGs).** Read counts were normalized by calculating the number of reads per kilobase per million reads (RPKM) for each transcript in individual samples using CLC Genomics Workbench software (version 11.0.1, Qiagen GmbH). DEGs were identified using fold change  $\geq 2$  or  $\leq -2$  filtering analysis with a false discovery rate (FDR) of  $P < 0.05$ . Gene expression was visualized using principal components analysis (PCA) plot and clustering heat map analyses. Volcano plots were used to visualize changes in gene expression between  $-\log_{10}$  P-value and  $\log_2$  fold change using CLC Genomics Workbench software (version 12.0, Qiagen GmbH).

**Functional enrichment analysis.** An unsupervised method for clustering genes into groups based on their expression pattern across all samples, K-means clustering and functional enrichment analysis of DEGs were visualized using integrated Differential Expression and Pathway analysis (iDEP) (bioinformatics.sdstate.edu/idep/) (20). Gene Ontology (GO) terms of biological process (<http://www.geneontology.org/>) and Kyoto Encyclopedia of Genes and Genomes (KEGG) pathway (<http://www.genome.jp/kegg/>) enrichment of DEGs between sample groups were analyzed and assigned using the web-based Enrichr suite software (maayanlab.cloud/Enrichr/) (21).

**Metabolome analysis.** Based on the results of transcriptomic analysis, mitochondrial and metabolic reprogramming was investigated. Metabolite extraction from the right heart of Su/Hx and Su/Hx + CH rats and metabolome analysis were performed according to Human Metabolome Technologies, Inc. Instructions, as previously described (Appendix S1) (22).

**Reverse transcription-quantitative (RT-q)PCR.** Total RNA from RV tissue was extracted using the Rneasy Fibrous Tissue

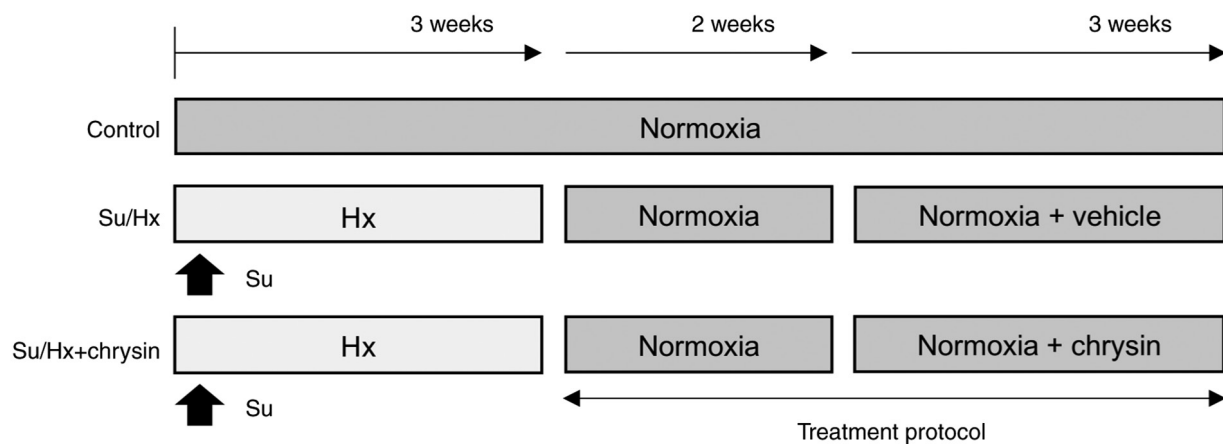


Figure 1. Timeline of experimental procedure. Su (20 mg/kg) was subcutaneously injected into 5-week-old male Sprague-Dawley rats. The rats were maintained under normobaric Hx (10% O<sub>2</sub>) for 3 weeks, then returned to normoxic conditions (21% O<sub>2</sub>) for 2 weeks. Chrysin administration commenced at the end of 2 week normoxic period and continued for 3 weeks. Su, SU5416; Hx, hypoxia.

kit and isolated RNA (0.2–0.5  $\mu$ g) was reverse-transcribed using an RT2 First Strand kit (both Qiagen GmbH) according to the manufacturer's instructions. qPCR was performed using SYBR<sup>®</sup> Green ROX qPCR Master Mix (Qiagen GmbH) in an ABI 7300 system (Applied Biosystems; Thermo Fisher Scientific, Inc.). RT2 First Strand kit (cat. no. 330404; Qiagen GmbH) were used to analyze expression of Ppar $\gamma$ , carnitine palmitoyl transferase 1 B (Cpt1b), cluster of differentiation 36 (Cd36), mitofusin1 (Mfn1), Mfn2, optic atrophy 1 (Opa1), mitochondrial transcription factor A (Tfam) and dynamin-related protein 1 (Drp1). The primers are listed in Appendix S2. PCR was performed as follows: 10 min at 95°C, followed by 40 cycles of 15 sec at 95°C and 1 min at 60°C. Data analysis was performed using the comparative C<sub>q</sub> method and ABI software (SDS version 1.4).  $\beta$ -actin was used for normalization of mRNA expression levels (23).

**Invasive right heart catheterization.** Pulmonary hemodynamics were measured in rats lightly anesthetized with isoflurane (4% for induction, 1–2% for maintenance) after blood pressure was measured. Anesthetized rats underwent tracheostomy and were placed on a ventilator (Harvard Apparatus). A 2.0-F microtip pressure transducer (Millar Instruments) was inserted into the RV. RV systolic pressure (SP), stroke volume, heart rate and differential of pressure with time (dP/dt) index were continuously monitored for >10 min and data were analyzed using a Power Lab system (AD Instruments). At the end of monitoring, arterial elastance (Ea) and end-systolic elastance (Ees) were measured with vena cava compression. Following hemodynamic measurement, rats were euthanized with pentobarbital sodium (150 mg/kg). Hearts were removed and the RV free wall was dissected from the left ventricle and septum (LV + S). The RV:LV + S weight was calculated as an index of RV hypertrophy. Sections of the right heart and lung were stored in RNAlater Tissue Reagent (Qiagen GmbH) and formalin for RT-qPCR and pathological analysis, respectively.

**Pathological analysis.** Paraffin-embedded RV and lung specimens were sectioned (3  $\mu$ m each). Myocyte cross-sectional area (CSA) was visualized using hematoxylin and eosin

(H&E) staining. H&E staining was performed with Mayer's Hematoxylin solution for 5 min and eosin solution (Muto Pure Chemical Co., Ltd.) for 2 min at room temperature. Images of H&E staining were captured and CSA was calculated using ImageJ software (version 1.53k; National Institutes of Health). A total of five sections were randomly selected from five rats/group. A total of  $\geq 30$  myocytes were observed/group. RV specimens were stained with Masson's trichrome stain. Masson's trichrome stain was performed with the mordant solution for 25 min, 0.75% orange G solution (Muto Pure Chemical Co., Ltd.) for 1 min, Masson B stain solution for 25 min, 2.5% phosphotungstic acid solution for 20 min, and aniline blue (Muto Pure Chemical Co., Ltd.) for 8 min at room temperature. The stained RV myocardial slides were observed in five randomly selected fields of view at 400x magnification. All slides were examined using a light microscope Eclipse 55i (Nikon Corporation).

The fibrotic area dyed blue was quantified using ImageJ. Lung specimens were stained with Elastica van Gieson (EVG) stain. EVG staining was performed with Maeda modified resorcin-fuchsin solution for 50 min, Weigert's Iron Hematoxylin Staining (both Muto Pure Chemical Co., Ltd.) for 10 min and Van Gieson Solution (FUJIFILM Wako Pure Chemical Co., Ltd.) for 2 min, at room temperature. The extent of pulmonary vessel luminal obstruction was evaluated as previously reported: Grade 0, no evidence of neointimal formation; grade 1, partial ( $\leq 50\%$ ) luminal occlusion; and grade 2, severe ( $> 50\%$ ) luminal occlusion. All pulmonary arteries (outer diameter,  $< 100 \mu$ m) in one section/animal were counted (14).

**Statistical analysis.** To assess differences between groups, unpaired two-tailed t-test and one-way ANOVA were used due to potential assumption violations (equal variance) when using more standard tests. When significant differences were detected, individual mean values were compared using post-hoc tests that allowed for multiple comparisons with adequate type I error control (Bonferroni). Statistical analysis was performed using GraphPad Prism version 9.1 (GraphPad Software, Inc.) Data are presented as the mean  $\pm$  SEM of  $\geq 3$  independent repeats.  $P < 0.05$  was considered to indicate a statistically significant difference.

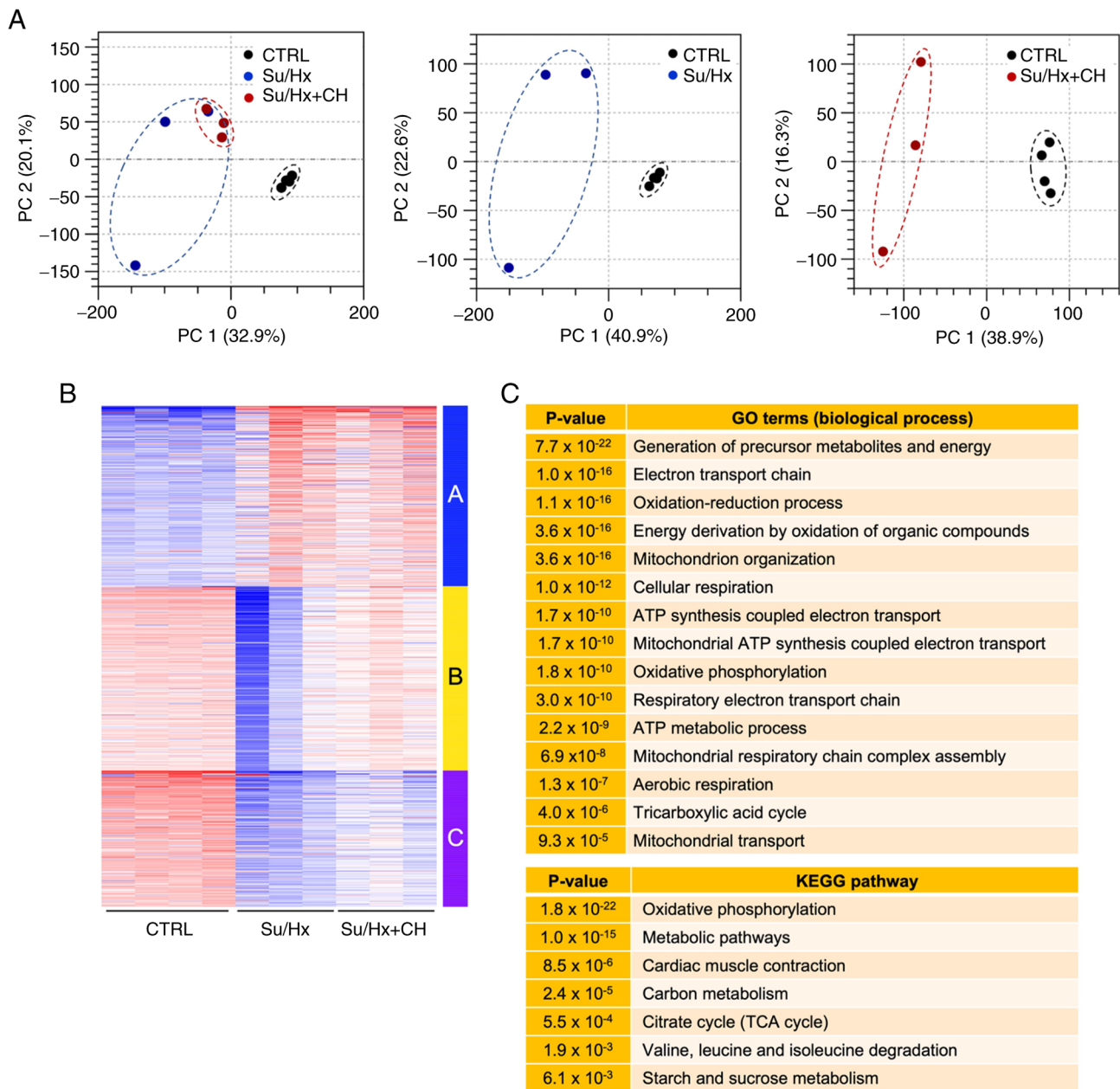


Figure 2. Analysis of right heart tissue transcriptome. (A) PCA of RNA-sequencing data. PC1 and 2 represent 32.9 and 20.1% (left), 40.9 and 22.6% (middle), and 38.9 and 16.3% (right) of total variation, respectively. Each dot denotes a single biological replicate; dashed circles represent three replicates/individual sample. (B) K-means clustering of 2,000 variable genes. Genes were classified based on similar expression patterns (red, high; white, intermediate; blue, low). Individual samples are displayed on the vertical axis, and genes on the horizontal axis. (C) Functional enrichment analysis of genes in Cluster B. Enriched GO terms associated with biological process and KEGG pathways. PCA, principal components analysis; GO, Gene Ontology; KEGG, Kyoto Encyclopedia of Genes and Genomes; CTRL, control; Su, SU5416; Hx, hypoxia; CH, chrysin.

## Results

**Transcriptomic changes in RV of Su/Hx + CH rats.** To determine CH-mediated alteration of gene expression in RV of Su/Hx rats, RNA-seq was used to analyze the transcriptome of heart tissue from CTRL, Su/Hx and Su/Hx + CH rats. PCA was performed to assess the reproducibility of biological replicates between CTRL, Su/Hx and Su/Hx + CH groups. Su/Hx and Su/Hx + CH samples were notably separated from CTRL samples (Fig. 2A). PCA plot showed that the Su/Hx + CH group was partially separated from the Su/Hx group.

K-means clustering of 2,000 variable genes was performed based on similar expression patterns (Fig. 2B). Cluster B,

expression of which was downregulated in Su/Hx and restored in the Su/Hx + CH group, was used for functional enrichment analysis (Fig. 2C). Compared with CTRL, downregulated genes in the Su/Hx group were associated with mitochondrial energy metabolism, such as ‘generation of precursor metabolites and energy’, ‘electron transport chain’, ‘mitochondrion organization’, ‘ATP synthesis coupled electron transport’, ‘mitochondrial ATP synthesis coupled electron transport’, ‘oxidative phosphorylation’ and ‘tricarboxylic acid cycle’, and these expression patterns were restored in Su/Hx + CH group. These results indicated that CH was involved in regulation of mitochondrial and metabolic gene expression in the RV of Su/Hx rats.



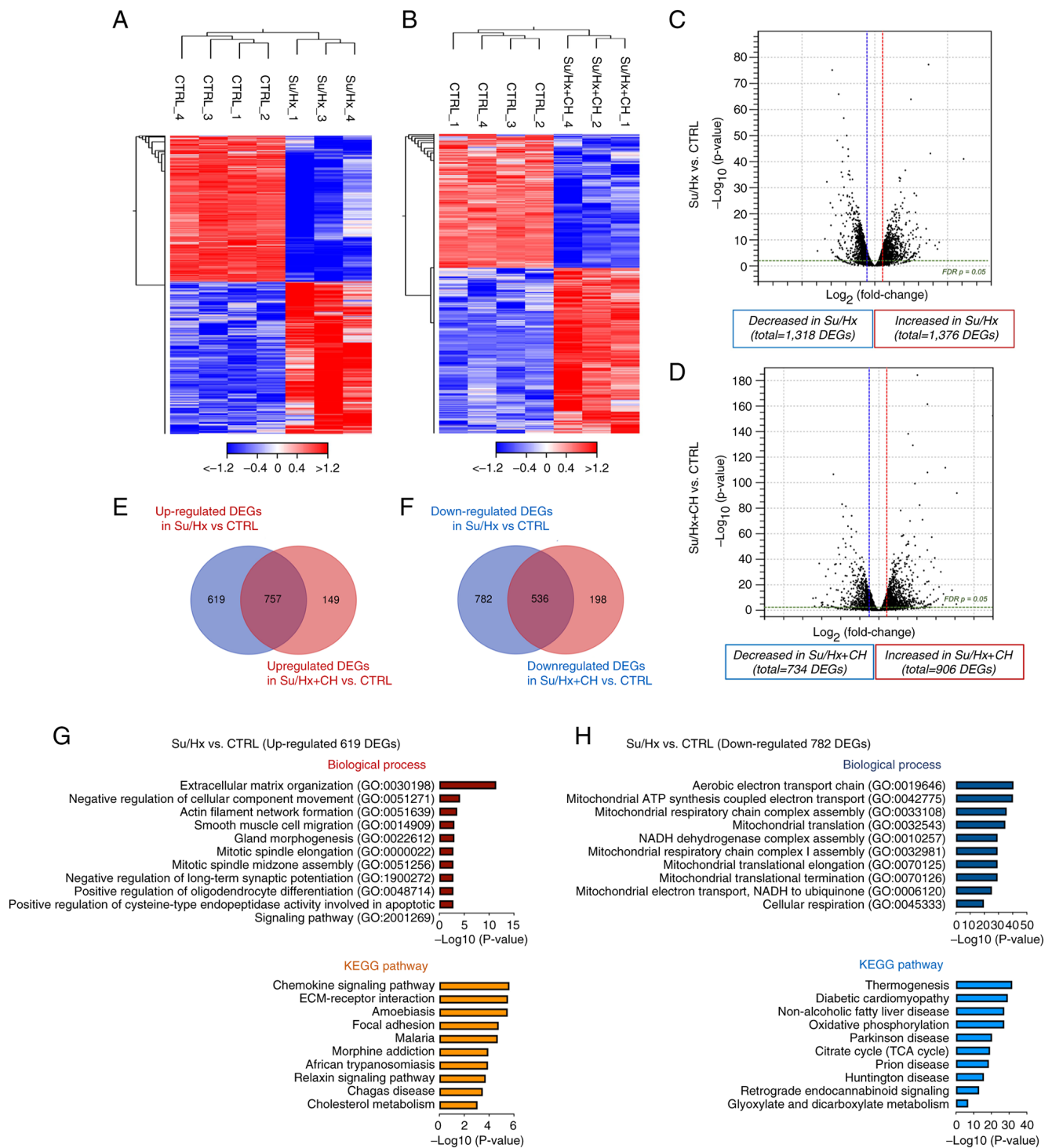


Figure 3. Expression profiling of right heart tissue. Hierarchical clustering of differential expression profiles between CTRL and (A) Su/Hx and (B) Su/Hx + CH. Individual samples are shown in columns, and genes in rows. Heatmaps represent relative expression (red, high; white, intermediate; blue, low). Volcano plots representing DEGs between CTRL and (C) Su/Hx and (D) Su/Hx + CH. Vertical lines,  $\log_2$  fold change  $\geq 2$  or  $\leq -2$ ; horizontal line, significance cut-off (false discovery rate,  $P=0.05$ ). Venn diagram identifying differences in (E) up- and (F) downregulated DEGs. (G) Functional enrichment analysis of 619 upregulated DEGs in Su/Hx vs. CTRL. Upregulated GO terms are hypothesized to be the disease etiology in the Su/Hx model and suppressed by CH. (H) Functional enrichment analysis of 782 downregulated DEGs in Su/Hx vs. CTRL. Downregulated GO terms are hypothesized to be the disease etiology in the Su/Hx model and restored by CH. CTRL, control; Su, SU5416; Hx, hypoxia; CH, chrysin; DEG, differentially expressed gene; GO, Gene Ontology; KEGG, Kyoto Encyclopedia of Genes and Genomes.

**DEG profiles.** Difference in RPKM was calculated and DEGs were identified using  $\text{FDR} < 0.05$  and fold change  $\geq 2$  or  $\leq -2$ . Compared with CTRL, hierarchical clustering analysis and volcano plot showed that 2,694 (1,376 up- and 1,318 downregulated) and 1,640 (906 up- and 734 downregulated) unique genes

were significantly changed in Su/Hx and Su/Hx + CH groups, respectively (Fig. 3A-D). DEGs in the Su/Hx and Su/Hx + CH groups were compared to identify genes upon which CH exerted cardioprotective effects. A total of 619 DEGs upregulated in Su/Hx but not Su/Hx + CH compared with CTRL

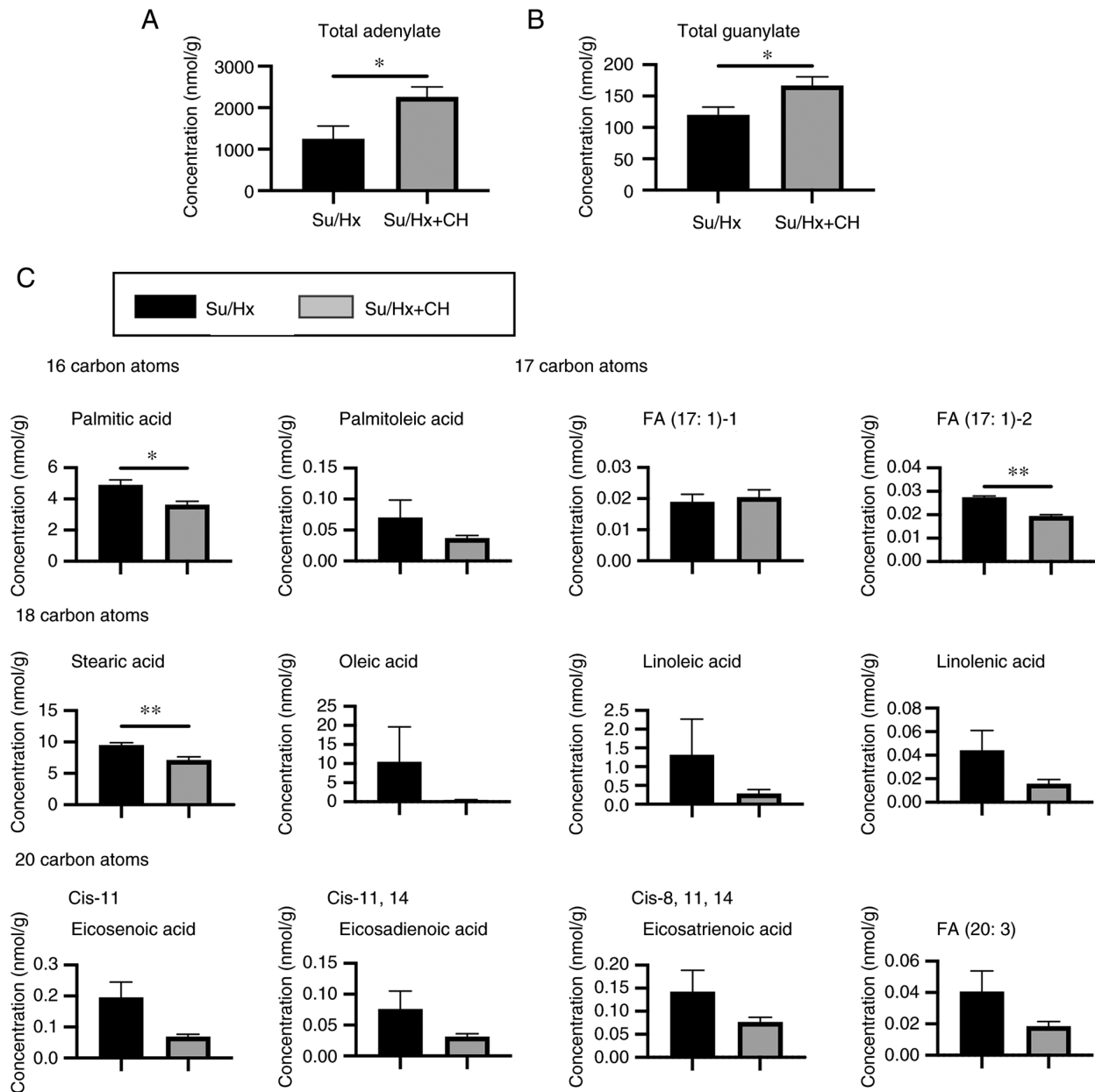


Figure 4. Metabolic analysis of the right heart. (A) Total concentration of adenylate (sum of AMP, ADP and ATP) was higher in Su/Hx + CH than Su/Hx. (B) Total concentration of guanylate (sum of GMP, GDP and GTP) was higher in Su/Hx + CH than Su/Hx. (C) Concentration of LCFAs with aliphatic tails of 16-20 carbons by liquid chromatography time-of-flight mass spectrometry. LCFAs, such as palmitic and stearic acids, were higher in Su/Hx than Su/Hx + CH. \* $P < 0.05$ , \*\* $P < 0.01$  vs. Su/Hx. LCFA, long-chain fatty acid; LC-TOFMS; Su, SU5416; Hx, hypoxia; CH, chrysin.

were identified (Fig. 3E). In addition, among transcripts, 1,318 DEGs in the Su/Hx group were downregulated relative to CTRL; of these, 782 transcripts were not downregulated in the Su/Hx + CH group (Fig. 3F).

To characterize the functional features of 619 up- and 782 downregulated DEGs in the Su/Hx group, enrichment analysis for GO annotation and KEGG pathway enrichment was performed. In biological process, the top ten terms were associated with cardiac fibrosis, such as 'extracellular matrix organization' (GO:0030198), 'negative regulation of cellular component movement' (GO:0051271) and 'actin smooth muscle migration' (GO:0014909; Fig. 3G). KEGG pathway analysis showed the terms 'chemokine signaling pathway', 'extracellular matrix-receptor interaction' and 'focal adhesion'. These results suggested that increased expression of

fibrosis- and inflammation-associated genes positively regulated RV dysfunction in Su/Hx rats and CH may protect against upregulation of these genes. Biological process mapping of 782 downregulated DEGs revealed significant association with mitochondrial function, including 'aerobic electron transport chain' (GO:0019646), 'mitochondrial ATP synthesis coupled electron transport' (GO:0042775), 'mitochondrial respiratory chain complex assembly' (GO:0033108) and 'mitochondrial translation' (GO:0032543) in the Su/Hx group (Fig. 3H). These data indicate that CH may improve mitochondrial biogenesis in the RV of Su/Hx PAH rats.

*Metabolic changes in right heart of Su/Hx + CH rats.* To evaluate whether CH affected cardiac metabolism in PAH, metabolic changes in the heart of Su/Hx rats in the

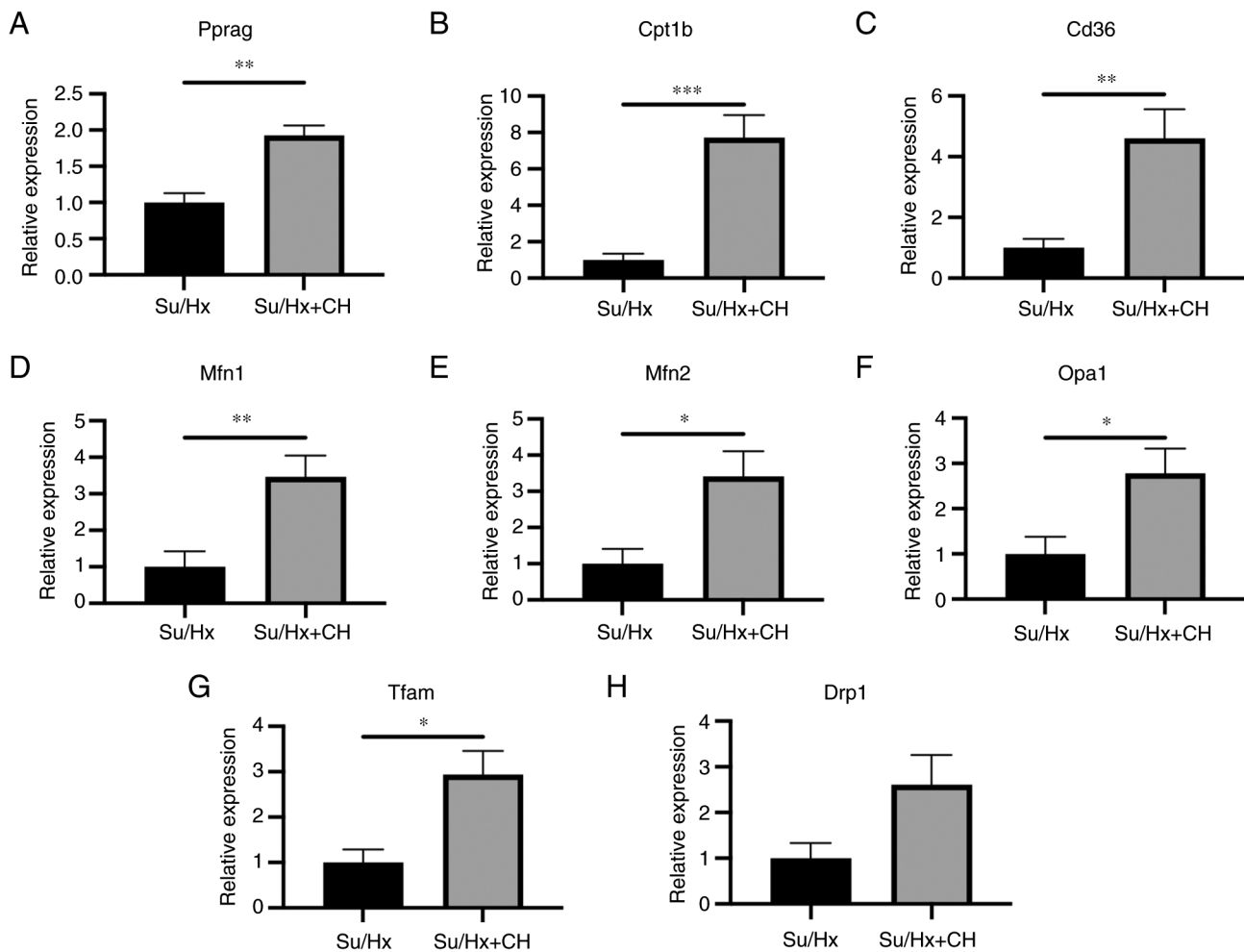


Figure 5. RT-qPCR analysis of right heart tissue. Genes associated with PPAR $\gamma$ , lipid metabolism and mitochondrial dynamics were analyzed using RT-qPCR in the right heart tissue. RNA expression levels of (A) Pparg, (B) Cd36 and (C) Cpt1b were higher in Su/Hx + CH than Su/Hx (fold regulation, 1.93, 4.61 and 7.73, respectively). Among genes associated with fusion and biogenesis dynamics, (D) Mfn1, (E) Mfn2, (F) Opa1 and (G) Tfam expression levels were higher in Su/Hx + CH than Su/Hx (fold regulation, 3.47, 3.41, 2.78 and 2.94, respectively). (H) No significant difference was observed between Su/Hx and Su/Hx + CH groups regarding Drp1 expression. \* $P < 0.05$ , \*\* $P < 0.01$ , \*\*\* $P < 0.001$  vs. Su/Hx. Cd36, cluster of differentiation 36; Cpt1b, carnitine palmitoyl transferase 1 B; Drp1, dynamin-related protein 1; Mfn, mitofusin; Opa1, optic atrophy 1; Pparg, peroxisome proliferator-activated receptor  $\gamma$ ; Tfam, mitochondrial transcription factor A; RT-q, reverse transcription-quantitative; Su, SU5416; Hx, hypoxia; CH, chrysin.

presence or absence of CH were determined via mass spectrometry-based metabolic analysis. After isotopic and fragment peaks were removed, capillary electrophoresis time-of-flight mass spectrometry detected peaks in all samples. These peaks were identified with metabolite standards by matching the  $m/z$  values and quantified using the normalized migration time. PC1 and PC2 of metabolites in ten samples accounted for 36.0 and 21.2% of total metabolites, respectively. However, PCA plots revealed that Su/Hx samples exhibited greater within-group variability than CH and overlapped with Su/Hx samples (Fig. S1A). By contrast, hierarchical heatmap clustering analysis showed that the biological replicates were separated between Su/Hx and Su/Hx + CH groups (Fig. S1B). These results indicated differences in the amounts of certain metabolites between the Su/Hx and Su/Hx + CH groups.

Whole glycolysis, lipid metabolism, and TCA cycle data are presented in Fig. S2. No significant differences were observed in glycolysis, TCA cycle, glutathione, NADH and NADPH, which indicated that the glycolytic metabolic

pathway was not significantly affected by CH. By contrast, the total concentration of adenylate was significantly higher in Su/Hx + CH than Su/Hx, indicating that CH improved energy production (Fig. 4A). Total concentration of guanylate was also significantly greater in Su/Hx + CH than Su/Hx (Fig. 4B). LC-TOFMS showed that concentration of long-chain fatty acids (LCFAs), such as palmitic acid/stearic acid, was higher in Su/Hx and lower in Su/Hx + CH (Fig. 4C).

**RT-qPCR analysis of right heart tissue.** Genes associated with mitochondrial energy production were analyzed using RT-qPCR in right heart tissue ( $n=5$ /group). RT-qPCR revealed that RNA expression of Pparg, Cd36 and Cpt1b in the Su/Hx + CH group was higher than in the Su/Hx group (fold regulation, 1.93, 4.61 and 7.73, respectively; Fig. 5A-C). RNA expression levels of genes associated with mitochondrial biogenesis, such as Mfn1, Mfn2, Opa1 and Tfam, were upregulated in Su/Hx + CH compared with Su/Hx (fold regulation, 3.47, 3.41, 2.78 and 2.94, respectively; Fig. 5D-G). No significant difference was observed between groups regarding RNA

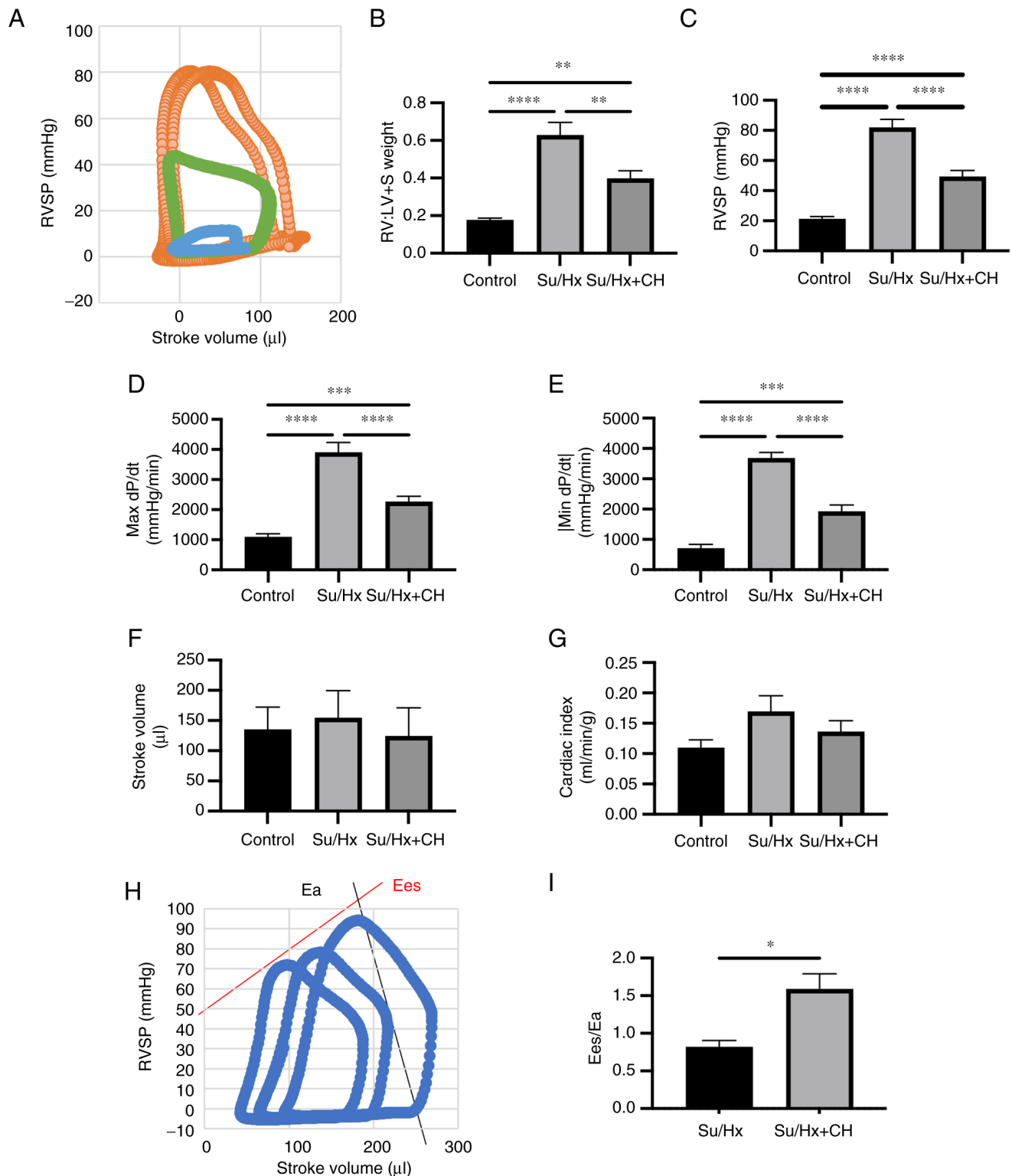


Figure 6. Hemodynamic analysis using Millar Mikro-Tip® catheter. (A) Representative pressure-volume curve. Orange, Su/Hx; green, Su/Hx + CH; blue, CTRL. (B) RV:LV + S weight. (C) RVSP, (D) max dP/dt, and (E) absolute value of min dP/dt were lower in Su/Hx + CH group than Su/Hx. (F) Stroke volume. (G) Cardiac index. (H) Calculation of Ea/Ees using pressure-volume curve. (I) Ea/Ees in Su/Hx and Su/Hx + CH. \* $P < 0.05$ , \*\* $P < 0.01$ , \*\*\* $P < 0.001$ , \*\*\*\* $P < 0.0001$ . Ea, arterial elastance; Ees, end-systolic elastance; LV + S, left ventricle + septum; RV, right ventricle; SP, systolic pressure; Su, SU5416; Hx, hypoxia; CH, chrysin; dP/dt, differential of pressure with time.

expression of genes associated with mitochondrial fission, such as Drp1 (fold regulation, 2.61; Fig. 5H).

*Hemodynamic analysis using Millar Mikro-Tip® catheter.* Hemodynamic parameters were measured using Millar

Mikro-Tip catheter system (n=5-8). Representative pressure-volume curve is presented in Fig. 6A. RV:LV + S was significantly lower in Su/Hx + CH than in Su/Hx (Fig. 6B). RVSP was  $82.0 \pm 5.5$  in Su/Hx and  $49.4 \pm 4.0$  mmHg in Su/Hx + CH (Fig. 6C). Maximum and minimum dP/dt, indices



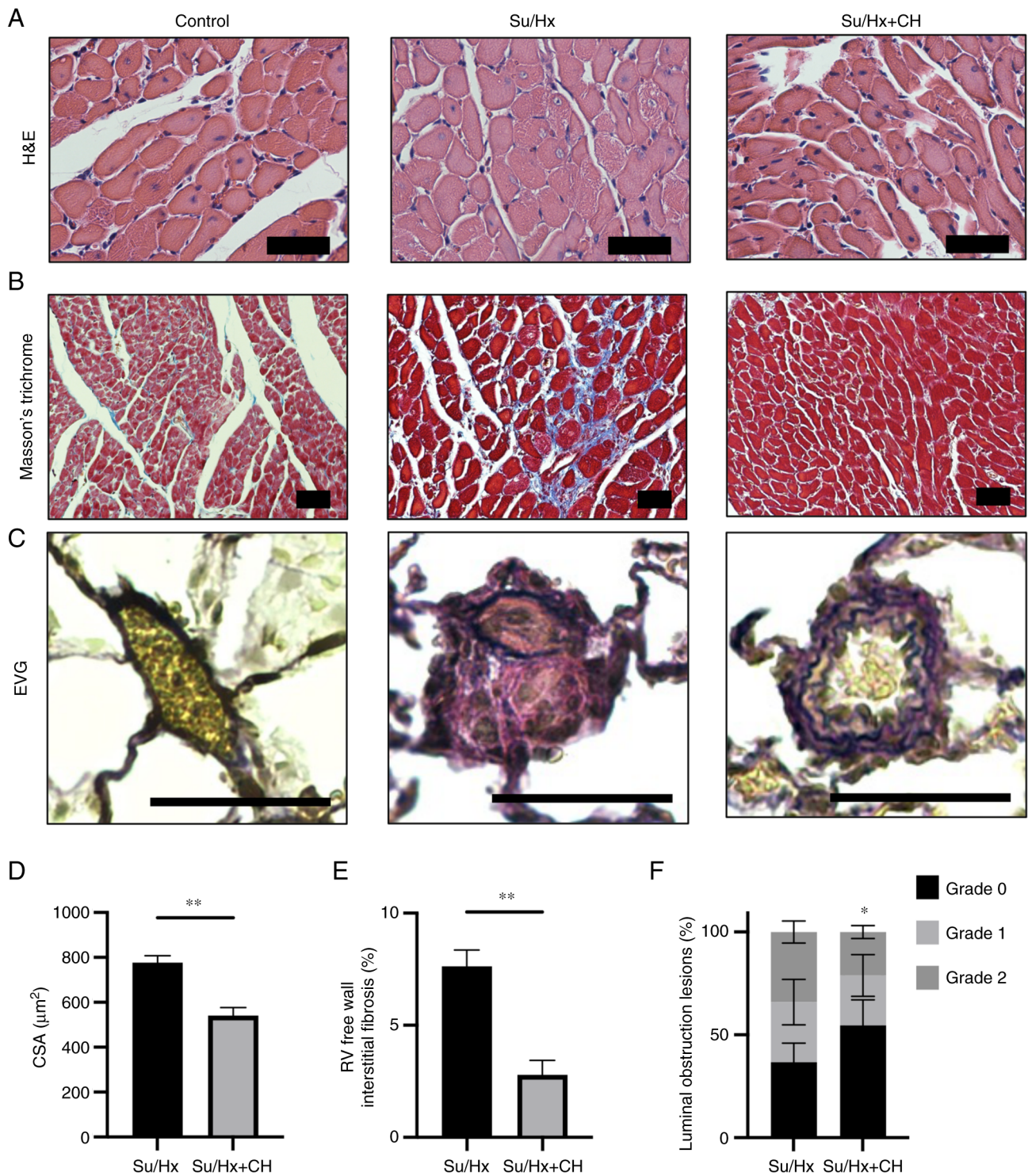


Figure 7. Histological analysis of right heart and pulmonary artery. Representative images of (A) H&E- and (B) Masson's trichrome-stained RV free wall and (C) EVG-stained pulmonary artery. Scale bar, 50  $\mu\text{m}$ . (D) Quantified cardiomyocyte CSA in H&E-stained section. RV free wall myocyte size was smaller in Su/Hx + CH than Su/Hx. (E) Quantified fibrosis area in Masson's trichrome-stained section. RV free wall fibrosis was higher in Su/Hx than Su/Hx + CH. (F) Quantified pulmonary artery remodeling index in EVG section. The extent of pulmonary vessel luminal obstruction in grade 2 was lower in Su/Hx + CH compared with Su/Hx. \* $P < 0.05$ , \*\* $P < 0.01$  vs. Su/Hx. CSA, cross-sectional area; EVG, Elastica van Gieson; H&E, hematoxylin and eosin; RV, right ventricle; Su, SU5416; Hx, hypoxia; CH, chrysin.

of RV systolic and diastolic performance, were lower in Su/Hx and higher in Su/Hx + CH (Fig. 6D-E). No significant differences were observed in stroke volume and cardiac index (Fig. 6F and G). Ees/Ea, a clinical index of ventricle-artery functional coupling, was higher in Su/Hx + CH than Su/Hx group (Fig. 6H and I).

**Histological analysis of right heart and pulmonary artery.** Myocyte CSA was visualized using H&E staining (Fig. 7A). The fibrotic area was stained blue using Masson's trichrome stain (Fig. 7B). RV free wall myocyte size was significantly smaller in Su/Hx + CH than Su/Hx (Fig. 7D), suggesting CH treatment may have ameliorated RV hypertrophy. RV free wall



fibrosis was significantly higher in Su/Hx than Su/Hx + CH (Fig. 7E), suggesting CH may have decreased RV wall fibrosis. Pulmonary artery remodeling was pathologically quantified using EVG staining (Fig. 7C). The extent of pulmonary vessel luminal obstruction in grade 2 was significantly lower in Su/Hx + CH compared with Su/Hx (Fig. 7F), suggesting CH alleviated pulmonary artery remodeling.

## Discussion

The present study investigated the molecular mechanisms underlying the effects of CH on RV remodeling and dysfunction in the development of PH. Gene expression changes in RV of Su/Hx rats in the presence or absence of CH were analyzed using RNA-seq. Furthermore, metabolomic profiling of RVs was used to determine metabolic regulation by CH and pathophysiological changes were observed in Su/Hx + CH rats. Transcriptome analysis suggested that pathways associated with mitochondrial energy metabolism were downregulated in Su/Hx and restored in Su/Hx + CH, such as generation of precursor metabolites and energy, mitochondrial ATP synthesis, oxidative phosphorylation and TCA cycle. CH protected against downregulation of these genes. Metabolome analysis revealed that CH increased the total concentration of adenylate, which suggested an improvement in whole energy production. CH decreased accumulation of LCFA. RT-qPCR revealed that expression of PPAR $\gamma$ , a master regulator of FA metabolism and mitochondrial biogenesis, was increased in RV of Su/Hx + CH rats. Genes associated with FA transport and mitochondrial biogenesis were also increased in the RV of Su/Hx + CH rats.

Regulation of mitochondrial biogenesis in the pulmonary vascular wall and RV is a therapeutic target in PH (24,25). RT-qPCR revealed that expression of PPAR $\gamma$  was increased in RV of Su/Hx + CH rats. PPAR $\gamma$ , a member of the nuclear hormone receptor superfamily, is ubiquitously expressed in myocardium, pulmonary vascular smooth muscle and endothelial cells and serves a key role in lipid metabolism and mitochondrial dynamics, resulting in inhibited ventricular hypertrophy (26-28). PPAR $\gamma$ -associated signaling is involved in multiple processes, including regulation of mitochondrial biogenesis, induction of antioxidant genes, transrepression of inflammatory signaling and regulation of Nitric oxide bioavailability in PH (29-33).

CH is a phytochemical categorized as a flavonoid based on its chemical structure. It is present in propolis, honey, passion fruit, mushrooms and other plant sources; it has been used to treat numerous types of degenerative disorder and exhibits anti-inflammatory activity (34-36). In addition, it has been used in the treatment of numerous types of metabolic malfunction, such as metabolic syndrome (37,38).

In rats exposed to chronic Hx, CH exhibits cardioprotective effects, such as antitumor and antioxidant effects, leading to prevention of vascular remodeling (9,39). To the best of our knowledge, however, its precise molecular effects on RV have not been defined. In a previous report, CH was shown to serve as a PPAR $\gamma$  agonist and directly upregulate transcriptional activity of PPAR $\gamma$  (40). Here, transcriptome analysis indicated that CH partially improved Su/Hx-induced downregulation of genes associated with mitochondrial function, such as aerobic electron transport chain, mitochondrial ATP synthesis-coupled

electron transport and mitochondrial respiratory chain complex assembly. Likewise, mitochondrial oxidative phosphorylation and TCA cycle downregulation in RV of Su/Hx rats was partly reversed by CH. CH may upregulate mitochondrial energy production, which is associated with an increase in total adenylate production. Improvement of energy production in mitochondria by upregulation of PPAR $\gamma$  may be a key treatment target of CH for RV dysfunction in PAH.

FA metabolic regulation in PH may be cell- and etiology-specific, thus complicating therapeutic targeting (41). In the Randle cycle, FA or glucose exhibit a negative regulatory association. FA and glucose oxidation share a reciprocal mechanism (42). Although FA oxidation is considered to account for a large part of cellular energy production in the RV, it has not been completely defined. RV-specific accumulation of increased LCFAs may be a hallmark of lipotoxicity (43,44). Here, CH upregulated gene expression of Cd36 and Cpt1b, which transport Fas across plasma and mitochondrial membranes (45,46). Moreover, metabolome analysis indicated that CH decreased accumulation of LCFAs in the RV, particularly palmitic and stearic acid. It was hypothesized that decreasing LCFA accumulation may be another mechanism by which CH improves RV remodeling.

The present study has certain limitations. The cardiovascular unit is composed of two primary functional units: RV and pulmonary vasculature. As right heart failure in PH is the consequence of increased afterload, a full understanding of physiological and pathobiological aspects in the cardiopulmonary unit is required to understand the molecular mechanisms underlying PH (47). Decreased oxidative phosphorylation and increased glycolysis are considered primary metabolic pathways disrupted in PH (48). Mitochondria in RV cardiomyocytes and pulmonary vascular cells may exhibit similar respiratory suppression followed by increased glucose uptake and glycolysis in PH. The complexities of metabolic reprogramming and mitochondrial dysfunction may promote cell survival and proliferation, while metabolic switching in pulmonary vascular cells may drive extensive remodeling, which has been proposed as a metabolic theory (48,49). The aforementioned studies suggest CH may act on both RV and pulmonary vasculature. The present study indicated that CH altered gene expression and mitochondrial metabolite levels in cardiomyocytes. However, whether these transcriptomic changes were solely due to the direct effects of CH on RV remains unclear as transcriptome analysis of resistant pulmonary blood vessels using laser microdissection (50) was not performed in this study.

The present study did not fully elucidate the mitochondrial dynamics. CH upregulated numerous mitochondrial fusion genes. Expression of DRP1, a representative fission marker, was higher in Su/Hx + CH than Su/Hx, although this was not statistically significant. For functional efficiency of DRP1, phosphorylation at the serine 616 residue is key in addition to the gene expression (51). However, protein level of phosphorylated DRP1 was not evaluated in the present study. Further investigation is needed to elucidate the effect of CH on mitochondrial dynamics.

CH has multiple effects, such as anti-oxidation and anti-inflammatory, in addition to aforementioned metabolic effects (9-11,34-38). The present transcriptome analysis did not reveal the anti-inflammatory effect of CH, which has

been previously reported (10,11). The mild effects of CH as a flavonoid (including anti-oxidation, anti-inflammatory and anti-diabetic effects) (52) may make it superior to selective synthetic agents; however, the entire potential mechanism and side effects of CH in PAH need to be clarified before approval as a therapeutic drug (9,10).

In conclusion, the present study suggested that CH altered gene expression and mitochondrial metabolite levels in cardiomyocytes, resulting in improved RV remodeling and dysfunction in a Su/Hx PAH rat model. CH may be a potential candidate for therapeutic options in PAH.

### Acknowledgements

The authors would like to thank Ms. Sumina Atarashi and Ms. Tomoko Misawa for technical advice and Ms. Chieko Handa for administrative support (all Department of Respiriology, Graduate School of Medicine, Chiba University).

### Funding

This study was supported by Japan. Agency for Medical Research and Development-Core Research for Evolution Science and Technology (grant no. 21gm1410010s0101), KAKENHI (grant no. 19H03664) and Intractable Respiratory Diseases and Pulmonary Hypertension Research Group, Ministry of Health, Labor and Welfare, Japan (grant no. 20FC1027).

### Availability of data and materials

The datasets generated and/or analyzed during the current study are available in the NCBI Gene Expression Omnibus database repository, [ncbi.nlm.nih.gov/geo](https://ncbi.nlm.nih.gov/geo) (accession no. GSE186989). Other datasets used and/or analyzed during the current study are available from the corresponding author on reasonable request.

### Authors' contributions

KT, SS, YK, JDK and YN were involved in study design and conceptualization. TK, AY, AN and TJS performed animal experiments. KT and JDK confirm the authenticity of all the raw data. TK and AN wrote the manuscript. KT, YK and JDK critically revised the manuscript. YK, YN and TS were involved in the interpretation of data and supervision of the study. All authors have read and approved the final manuscript.

### Ethics approval and consent to participate

All animal procedures were approved by the Review Board for Animal Experiments of Chiba University (approval no. 30-126) and performed in accordance with the guidelines of the Animal Research Committee of Laboratory Animal Center, Graduate School of Medicine, Chiba University.

### Patient consent for publication

Not applicable.

### Competing interests

The authors declare they have no competing interests.

### References

- Voelkel NF, Quaife RA, Leinwand LA, Barst RJ, McGoon MD, Meldrum DR, Dupuis J, Long CS, Rubin LJ, Smart FW, *et al*: Right ventricular function and failure: Report of a national heart, lung, and blood institute working group on cellular and molecular mechanisms of right heart failure. *Circulation* 114: 1883-1891, 2006.
- Tonelli AR, Arelli V, Minai OA, Newman J, Bair N, Heresi GA and Dweik RA: Causes and circumstances of death in pulmonary arterial hypertension. *Am J Respir Crit Care Med* 188: 365-369, 2013.
- Frieler RA and Mortensen RM: Immune cell and other noncardiomyocyte regulation of cardiac hypertrophy and remodeling. *Circulation* 131: 1019-1030, 2015.
- Bishop SP and Altschuld RA: Increased glycolytic metabolism in cardiac hypertrophy and congestive failure. *Am J Physiol* 218: 153-159, 1970.
- Partovian C, Adnot S, Eddahibi S, Teiger E, Levame M, Dreyfus P, Raffestin B and Frelin C: Heart and lung VEGF mRNA expression in rats with monocrotaline- or hypoxia-induced pulmonary hypertension. *Am J Physiol* 275: H1948-H1956, 1998.
- Oikawa M, Kagaya Y, Otani H, Sakuma M, Demachi J, Suzuki J, Takahashi T, Nawata J, Ido T, Watanabe J and Shirato K: Increased [18F]fluorodeoxyglucose accumulation in right ventricular free wall in patients with pulmonary hypertension and the effect of epoprostenol. *J Am Coll Cardiol* 45: 1849-1855, 2005.
- Panche AN, Diwan AD and Chandra SR: Flavonoids: An overview. *J Nutr Sci* 5: e47, 2016.
- García-Lafuente A, Guillaumon E, Villares A, Rostagno MA and Martínez JA: Flavonoids as anti-inflammatory agents: Implications in cancer and cardiovascular disease. *Inflamm Res* 58: 537-552, 2009.
- Li XW, Wang XM, Li S and Yang JR: Effects of chrysin (5,7-dihydroxyflavone) on vascular remodeling in hypoxia-induced pulmonary hypertension in rats. *Chin Med* 10: 4, 2015.
- Yang M, Xiong J, Zou Q, Wang DD and Huang CX: Chrysin attenuates interstitial fibrosis and improves cardiac function in a rat model of acute myocardial infarction. *J Mol Histol* 49: 555-565, 2018.
- Kseibati MO, Sharawy MH and Salem HA: Chrysin mitigates bleomycin-induced pulmonary fibrosis in rats through regulating inflammation, oxidative stress, and hypoxia. *Int Immunopharmacol* 89: 107011, 2020.
- Abe K, Toba M, Alzoubi A, Ito M, Fagan KA, Cool CD, Voelkel NF, McMurtry IF and Oka M: Formation of plexiform lesions in experimental severe pulmonary arterial hypertension. *Circulation* 121: 2747-2754, 2010.
- Oka M, Homma N, Taraseviciene-Stewart L, Morris KG, Kraskauskas D, Burns N, Voelkel NF and McMurtry IF: Rho kinase-mediated vasoconstriction is important in severe occlusive pulmonary arterial hypertension in rats. *Circ Res* 100: 923-929, 2007.
- Toba M, Alzoubi A, O'Neill KD, Gairhe S, Matsumoto Y, Oshima K, Abe K, Oka M and McMurtry IF: Temporal hemodynamic and histological progression in Sugen5416/hypoxia/normoxia-exposed pulmonary arterial hypertensive rats. *Am J Physiol Heart Circ Physiol* 306: H243-H250, 2014.
- Taraseviciene-Stewart L, Kasahara Y, Alger L, Hirth P, Mc Mahon G, Waltenberger J, Voelkel NF and Tuder RM: Inhibition of the VEGF receptor 2 combined with chronic hypoxia causes cell death-dependent pulmonary endothelial cell proliferation and severe pulmonary hypertension. *FASEB J* 15: 427-438, 2001.
- Sanada TJ, Hosomi K, Shoji H, Park J, Naito A, Ikubo Y, Yanagisawa A, Kobayashi T, Miwa H, Suda R, *et al*: Gut microbiota modification suppresses the development of pulmonary arterial hypertension in an SU5416/hypoxia rat model. *Pulm Circ* 10: 2045894020929147, 2020.
- Guidelines of the Animal Research Committee of Laboratory Animal Center, Graduate School of Medicine, Chiba University. <https://www.chiba-u.ac.jp/general/JoureiV5HTMLContents/act/frame/frame110000180.htm>. Accessed March 3, 2022.

18. Kato F, Sakao S, Takeuchi T, Suzuki T, Nishimura R, Yasuda T, Tanabe N and Tatsumi K: Endothelial cell-related autophagic pathways in Sugen/hypoxia-exposed pulmonary arterial hypertensive rats. *Am J Physiol Lung Cell Mol Physiol* 313: L899-L915, 2017.
19. Takeuchi T, Sakao S, Kato F, Naito A, Jujo T, Yasuda T, Tanabe N and Tatsumi K: Pulmonary haemodynamics are correlated with intimal lesions in a rat model of severe PAH: Attenuation of pulmonary vascular remodelling with ambrisentan. *Histol Histopathol* 31: 1357-1365, 2016.
20. Ge SX, Son EW and Yao R: iDEP: An integrated web application for differential expression and pathway analysis of RNA-Seq data. *BMC Bioinformatics* 19: 534, 2018.
21. Kuleshov MV, Jones MR, Rouillard AD, Fernandez NF, Duan Q, Wang Z, Koplev S, Jenkins SL, Jagodnik KM, Lachmann A, *et al*: Enrichr: A comprehensive gene set enrichment analysis web server 2016 update. *Nucleic Acids Res* 44: W90-W97, 2016.
22. Sakao S, Kawakami E, Shoji H, Naito A, Miwa H, Suda R, Sanada TJ, Tanabe N and Tatsumi K: Metabolic remodeling in the right ventricle of rats with severe pulmonary arterial hypertension. *Mol Med Rep* 23: 227, 2021.
23. Livak KJ and Schmittgen TD: Analysis of relative gene expression data using real-time quantitative PCR and the 2(-Delta Delta C(T)) method. *Methods* 25: 402-408, 2001.
24. Yeligar SM, Kang BY, Bijli KM, Kleinhenz JM, Murphy TC, Torres G, San Martin A, Sutliff RL and Hart CM: PPAR $\gamma$  regulates mitochondrial structure and function and human pulmonary artery smooth muscle cell proliferation. *Am J Respir Cell Mol Biol* 58: 648-657, 2018.
25. Gomez-Arroyo J, Mizuno S, Szczepanek K, Van Tassell B, Natarajan R, dos Remedios CG, Drake JJ, Farkas L, Kraskauskas D, Wijesinghe DS, *et al*: Metabolic gene remodeling and mitochondrial dysfunction in failing right ventricular hypertrophy secondary to pulmonary arterial hypertension. *Circ Heart Fail* 6: 136-144, 2013.
26. Vidal-Puig AJ, Considine RV, Jimenez-Liñan M, Werman A, Pories WJ, Caro JF and Flier JS: Peroxisome proliferator-activated receptor gene expression in human tissues. Effects of obesity, weight loss, and regulation by insulin and glucocorticoids. *J Clin Invest* 99: 2416-2422, 1997.
27. Qi HP, Wang Y, Zhang QH, Guo J, Li L, Cao YG, Li SZ, Li XL, Shi MM, Xu W, *et al*: Activation of peroxisome proliferator-activated receptor  $\gamma$  (PPAR $\gamma$ ) through NF- $\kappa$ B/Brg1 and TGF- $\beta$ 1 pathways attenuates cardiac remodeling in pressure-overloaded rat hearts. *Cell Physiol Biochem* 35: 899-912, 2015.
28. Lee TW, Bai KJ, Lee TI, Chao TF, Kao YH and Chen YJ: PPARs modulate cardiac metabolism and mitochondrial function in diabetes. *J Biomed Sci* 24: 5, 2017.
29. Dominy JE and Puigserver P: Mitochondrial biogenesis through activation of nuclear signaling proteins. *Cold Spring Harb Perspect Biol* 5: a015008, 2013.
30. Fan W and Evans R: PPARs and ERRs: Molecular mediators of mitochondrial metabolism. *Curr Opin Cell Biol* 33: 49-54, 2015.
31. Ricote M and Glass CK: PPARs and molecular mechanisms of transrepression. *Biochim Biophys Acta* 1771: 926-935, 2007.
32. Calnek DS, Mazzella L, Roser S, Roman J and Hart CM: Peroxisome proliferator-activated receptor gamma ligands increase release of nitric oxide from endothelial cells. *Arterioscler Thromb Vasc Biol* 23: 52-57, 2003.
33. Pascual G, Fong AL, Ogawa S, Gamliel A, Li AC, Perissi V, Rose DW, Willson TM, Rosenfeld MG and Glass CK: A SUMOylation-dependent pathway mediates transrepression of inflammatory response genes by PPAR-gamma. *Nature* 437: 759-763, 2005.
34. Del Fabbro L, Rossito Goes A, Jesse CR, de Gomes MG, Cattelan Souza L, Lobo Ladd FV, Lobo Ladd AAB, Nunes Arantes RV, Reis Simionato A, Oliveira MS, *et al*: Chrysin protects against behavioral, cognitive and neurochemical alterations in a 6-hydroxydopamine model of Parkinson's disease. *Neurosci Lett* 706: 158-163, 2019.
35. Jiang Y, Gong FL, Zhao GB and Li J: Chrysin suppressed inflammatory responses and the inducible nitric oxide synthase pathway after spinal cord injury in rats. *Int J Mol Sci* 15: 12270-12279, 2014.
36. Tang H, Tao A, Song J, Liu Q, Wang H and Rui T: Doxorubicin-induced cardiomyocyte apoptosis: Role of mitofusin 2. *Int J Biochem Cell Biol* 88: 55-59, 2017.
37. Yamamoto Y: Effects of dietary chrysin supplementation on blood pressure and oxidative status of rats fed a high-fat high-sucrose diet. *Food Sci Technol Res* 20: 295-300, 2014.
38. Andrade N, Andrade S, Silva C, Rodrigues I, Guardão L, Guimarães JT, Keating E and Martel F: Chronic consumption of the dietary polyphenol chrysin attenuates metabolic disease in fructose-fed rats. *Eur J Nutr* 59: 151-165, 2020.
39. Fu B, Xue J, Li Z, Shi X, Jiang BH and Fang J: Chrysin inhibits expression of hypoxia-inducible factor-1 $\alpha$  through reducing hypoxia-inducible factor-1 $\alpha$  stability and inhibiting its protein synthesis. *Mol Cancer Ther* 6: 220-226, 2007.
40. Liang YC, Tsai SH, Tsai DC, Lin-Shiau SY and Lin JK: Suppression of inducible cyclooxygenase and nitric oxide synthase through activation of peroxisome proliferator-activated receptor-gamma by flavonoids in mouse macrophages. *FEBS Lett* 496: 12-18, 2001.
41. Xu W, Janocha AJ and Erzurum SC: Metabolism in pulmonary hypertension. *Annu Rev Physiol* 83: 551-576, 2021.
42. Randle PJ, Garland PB, Hales CN and Newsholme EA: The glucose fatty-acid cycle. Its role in insulin sensitivity and the metabolic disturbances of diabetes mellitus. *Lancet* 1: 785-789, 1963.
43. Brittain EL, Talati M, Fessel JP, Zhu H, Penner N, Calcutt MW, West JD, Funke M, Lewis GD, Gerszten RE, *et al*: Fatty acid metabolic defects and right ventricular lipotoxicity in human pulmonary arterial hypertension. *Circulation* 133: 1936-1944, 2016.
44. Hemnes AR, Brittain EL, Trammell AW, Fessel JP, Austin ED, Penner N, Maynard KB, Gleaves L, Talati M, Absi T, *et al*: Evidence for right ventricular lipotoxicity in heritable pulmonary arterial hypertension. *Am J Respir Crit Care Med* 189: 325-334, 2014.
45. Kampf JP and Kleinfeld AM: Is membrane transport of FFA mediated by lipid, protein, or both? An unknown protein mediates free fatty acid transport across the adipocyte plasma membrane. *Physiology (Bethesda)* 22: 7-14, 2007.
46. McGarry JD and Brown NF: The mitochondrial carnitine palmitoyltransferase system. From concept to molecular analysis. *Eur J Biochem* 244: 1-14, 1997.
47. Vonk Noordegraaf A, Chin KM, Haddad F, Hassoun PM, Hemnes AR, Hopkins SR, Kawut SM, Langleben D, Lumens J and Naeije R: Pathophysiology of the right ventricle and of the pulmonary circulation in pulmonary hypertension: An update. *Eur Respir J* 53: 1801900, 2019.
48. Ryan JJ and Archer SL: Emerging concepts in the molecular basis of pulmonary arterial hypertension: Part I: Metabolic plasticity and mitochondrial dynamics in the pulmonary circulation and right ventricle in pulmonary arterial hypertension. *Circulation* 131: 1691-1702, 2015.
49. Han S and Chandel NS: Lessons from cancer metabolism for pulmonary arterial hypertension and fibrosis. *Am J Respir Cell Mol Biol* 65: 134-145, 2021.
50. Laumanns IP, Fink L, Wilhelm J, Wolff JC, Mitnacht-Kraus R, Graef-Hoechst S, Stein MM, Bohle RM, Klepetko W, Hoda MA, *et al*: The noncanonical WNT pathway is operative in idiopathic pulmonary arterial hypertension. *Am J Respir Cell Mol Biol* 40: 683-691, 2009.
51. Kar UP, Dey H and Rahaman A: Regulation of dynamin family proteins by post-translational modifications. *J Biosci* 42: 333-344, 2017.
52. Naz S, Imran M, Rauf A, Orhan IE, Shariati MA, Ihtisham-Ul-H, IqraYasmin, Shahbaz M, Qaisrani TB, Shah ZA, *et al*: Chrysin: Pharmacological and therapeutic properties. *Life Sci* 235: 116797, 2019.



This work is licensed under a Creative Commons Attribution-NonCommercial-NoDerivatives 4.0 International (CC BY-NC-ND 4.0) License.